(*22*). More recently, a fatty acid amide isolated from bovine mesentery was found to be angiogenic (*23*), and synthetic arachidonamide was found to inhibit leukotriene biosynthesis (*24*). Our results raise the possibility that anandamide is formed via an as-yet-uncharacterized route of arachidonic acid metabolism leading to compounds that act, at least in part, through the cannabinoid receptor.

Finally, our results may help to clarify the biological significance of previously reported interactions between cannabinoids and eicosanoids (*25*).

REFERENCES AND NOTES

1. Y. Gaoni and R. Mechoulam, *J. Am. Chem. Soc.* **86**, 1646 (1964).
2. W. A. Devane, F. A. Dysarz III, M. R. Johnson, L. S. Melvin, A. C. Howlett, *Mol. Pharmacol.* **34**, 605 (1988); W. A. Devane, thesis, St. Louis University, St. Louis, MO, (1989).
3. L. A. Matsuda, S. J. Lolait, M. J. Brownstein, A. C. Young, T. I. Bonner, *Nature* **346**, 561 (1990).
4. C. M. Gérard, C. Mollereau, G. Vassart, M. Parmentier, *Biochem. J.* **279**, 129 (1991).
5. M. Herkenham *et al.*, *Proc. Natl. Acad. Sci. U.S.A.* **87**, 1932 (1990); M. Herkenham *et al.*, *J. Neurosci.* **11**, 563 (1991).
6. R. G. Pertwee, *Pharmacol. Ther.* **36**, 189 (1988).
7. R. Mechoulam *et al.*, *Experientia* **44**, 762 (1988); R. Mechoulam, W. A. Devane, R. Glaser, in *Marijuana/Cannabinoids: Neurobiology and Neurophysiology*, L. Murphy and A. Bartke, Eds. (CRC Press, Boca Raton, FL, 1992), pp. 1–33.
8. W. A. Devane *et al.*, *J. Med. Chem.* **35**, 2065 (1992).
9. Porcine brains were homogenized in chloroform and/or methanol and centrifuged at 13,000*g*. The organic solvent extract was fractionated over a silica column (70 to 230 μm, Kieselgel 60, Merck), according to elution schemes used to separate the major classes of lipids [C. C. Sweeley, *Methods Enzymol.* **14**, 254 (1969); J. C. Dittmer and M. A. Wells, *ibid.*, p. 482].
10. The TLC plates (analytical, RP-18, Merck) were eluted with methanol-dichloromethane (4:1) and developed twice. The first solvent front was at 3.1 cm, and the second was at 7.4 cm. The R_f value was 0.65 [W. A. Devane, L. Hanuš, R. Mechoulam, *Proceedings of the Fifth Nordic Neuroscience Meeting*, Publ. Univ. Kuopio Med. (1991), p. 198]. Anandamide eluted from a silica column (Kieselgel 60, 40 to 63 μm, Merck) with methanol-chloroform (2:98). It eluted from a reversed-phase column (RP-C_{18}, 40 to 63 μm, Sigma) with methanol-water (88:12).
11. The term "anandamide" was coined from the Sanskrit word "ananda," meaning bliss, and from the chemical nature of the compound.
12. GC-MS analyses were carried out with a Finnigan ITS-40 system and with a Finnigan TSQ-70B triple-stage quadrupole mass spectrometer coupled to a Varian 3400 gas chromatograph. Separations were performed on a DB-5 (0.25-μm film) capillary column that was 30 m in length and had an internal diameter (i.d.) of 0.25 mm. The column temperature was programmed to increase from 60 to 280°C at a rate of 20°C per minute. The compounds were injected into the GC in methylene chloride. The electron energy in EI measurements was 70 eV with one scan per second. The isobutane DCI measurements were carried out with a TSQ-70B mass spectrometer under standard conditions. High-resolution mass spectral measurements were performed with a Varian-MAT 711 double-focusing mass spectrometer. The CID measurements were carried out with the TSQ-70B triple-stage mass spectrometer. The collision energy was 50 eV, and argon was used as the target gas at an indicated pressure of 0.4 mtorr.
13. R. G. Pertwee, L. A. Stevenson, D. B. Elrick, R. Mechoulam, A. D. Corbett, *Br. J. Pharmacol.* **105**, 980 (1992).
14. The GC-MS and CID measurements of the TMS derivative of anandamide gave m/z 419 M^+ and 404 $[M\text{-}CH_3]^+$ fragment ions, which indicated formation of a mono-TMS ether. The CID spectrum of the m/z 404 ion exhibited two major fragment ions at m/z 118 and 172, corresponding to $Me_2Si^+OCH_2CH_2NH_2$ and $Me_2Si^+OCH_2CH_2NHCOCH{=}CH_2$, respectively.
15. W. A. Devane *et al.*, unpublished data.
16. H. Wenker, *J. Am. Chem. Soc.* **57**, 1079 (1935).
17. The one- and two-dimensional proton NMR spectra (in $CDCl_3$) were obtained on a Varian VXR300s spectrometer equipped with a 5-mm computer switchable probehead and on an AMX 400.133 Bruker spectrometer with a 5-mm reverse probehead. The chemical shifts are presented in parts per million. The Bruker library program (NOESY) was used for the two-dimensional measurements.
18. W. W. Christie, *Lipid Analysis* (Pergamon, Oxford, ed. 2, 1982), pp. 81–82; D. J. Frost and J. Barzilay, *Anal. Chem.* **43**, 1316 (1971).
19. Arachidonyl chloride, which was prepared from arachidonic acid and oxalyl chloride according to a published procedure (*24*), was dissolved in methylene chloride and added at 0°C under a nitrogen atmosphere to ethanolamine. The ethanolamine was present in a tenfold molar excess and was also dissolved in methylene chloride. After 15 min the reaction mixture was washed with water, dried, and the product purified by silica column chromatography (eluted with 2% methanol in chloroform) to give arachidonylethanolamide (an oil, ~90% yield) that was 97% pure as judged by GC-MS.
20. A. C. Howlett, D. M. Evans, D. B. Houston, in *Marijuana/Cannabinoids: Neurobiology and Neurophysiology*, L. Murphy and A. Bartke, Eds. (CRC Press, Boca Raton, FL, 1992), pp. 35–72.
21. F. A. Kuehl, Jr., T. A. Jacob, O. H. Ganley, R. E. Osmond, M. A. P. Meisinger, *J. Am. Chem. Soc.* **79**, 5577 (1957).
22. N. R. Bachur, K. Masek, K. L. Melmon, S. Udenfriend, *J. Biol. Chem.* **240**, 1019 (1965).
23. K. Wakamatsu, T. Masaki, F. Itoh, K. Kondo, K. Sudo, *Biochem. Biophys. Res. Commun.* **168**, 423 (1990).
24. E. J. Corey, J. R. Cashman, S. S. Kantner, S. W. Wright, *J. Am. Chem. Soc.* **106**, 1503 (1984).
25. S. H. Burstein, in (*20*), pp. 73–91 and references therein; R. G. Pertwee, *ibid.*, pp. 165–218; J. W. Fairbairn and J. T. Pickens, *Br. J. Pharmacol.* **72**, 401 (1981); A. Sklenovsky, J. Navratil, Z. Chmela, Z. Krejči, L. Hanuš, *Acta Univ. Palacki. Olomuc. Fac. Med.* **122**, 83 (1989).
26. P. J. Munson and D. Rodbard, *Anal. Biochem.* **107**, 220 (1980).

27. Supported by grants to R.M. from the National Institute for Drug Abuse (DA 6481) and the Amdursky Fund of the Friends of the Hebrew University and by a grant to R.G.P. from the Wellcome Trust. We thank I. Ringel (Jerusalem) for the initial NMR work, S. Levin (Jerusalem) for advice on chromatography, and J. Katzir and A. Idina (Haifa) for dedicated technical help.

1 September 1992; accepted 6 November 1992

Direct Visualization of the Dendritic and Receptive Fields of Directionally Selective Retinal Ganglion Cells

Guang Yang and Richard H. Masland*

Optical methods were used to locate the cell bodies of directionally selective ganglion cells in isolated rabbit retinas. These neurons detect the direction in which images move across the retinal surface and transmit that information to the brain. The receptive field of each identified cell was determined, after which the cell was injected with Lucifer yellow. An image of the receptive field border was then projected onto the fluorescent image of the dendrites, allowing precise comparison between them. The size of the receptive field matched closely the size of the dendritic arbor of that cell. This result restricts the types of convergence that can be postulated in modeling the mechanism of retinal directional selectivity.

A classic problem in the study of neural microcircuitry and neural computation is the mechanism by which directionally selective (DS) ganglion cells interpret inputs from preceding retinal neurons to deduce the direction of movement of a visual image formed on the retina (*1–3*). The relatively simple neural circuitry involved and the specific and clear function performed by DS cells have made this problem attractive for computational modeling. However, the modeling has been based on sparse biological facts. The input-output relations of the DS cells have been studied in detail and their dendritic morphology has been established (*4*), but the neural circuits that converge on the DS cells to create directional selectivity are unknown.

Cholinergic inputs from the starburst amacrine cells monosynaptically excite the DS ganglion cells (*5*, *6*). The starburst amacrine cells have widely spreading dendritic fields, which overlap extensively (*7*). Because a DS cell receives inputs from many starburst amacrine cells, the receptive field of each DS cell should cover an area considerably wider than the dendritic arbor

Program in Neuroscience and the Department of Neurosurgery, Harvard Medical School, Massachusetts General Hospital, Boston, MA 02114.

*To whom correspondence should be addressed.

of that cell. Alternatively, some other mechanism must exist to counteract the tendency of convergence to extend the receptive field. The relative size of the dendritic and receptive fields is thus critical for understanding the mechanism of directional selectivity.

We describe an approach that permitted a direct comparison between the receptive and dendritic fields of DS cells. The cell bodies of DS ganglion cells were fluorescently labeled in living retinas. Action potentials were then recorded, and the cells were studied morphologically by the injection of dye. The retrograde fluorescent tracer Fast blue (Sigma) was injected [10 μl of a 1% (w/v) solution] into the optic nerve of New Zealand White rabbits. After 2 to 3 days, the dark-adapted retina was isolated from the eye in oxygenated Ames medium (Sigma). A small piece of the retina was removed and then mounted on a piece of filter paper, with the ganglion cell layer up (8). A hole cut in the center of the filter paper allowed the projection of light stimuli onto the photoreceptors from below. The retina was held down by a nylon meshwork at the bottom of a perfusion chamber at 35°C. The chamber was placed on the stage of a fluorescence microscope. To prevent photodamage and bleaching of the photoreceptors caused by the ultraviolet (UV) illumination, we initially used an intensified video camera to view the Fast blue–labeled cells with minimum intensity and exposure. In the later experiments, we obtained similar results by using an electronic shutter gated by a foot pedal to control short exposures of the exciting light.

Under visual guidance, a tungsten-in-glass electrode (tip size, 10 to 20 μm; resistance, about 1 megohm) was advanced toward labeled cells (Fig. 1A). The DS cells could be tentatively identified by the appearance of their somata, which were medium to large and had a smooth outline. When the electrode was close to the cell body, large action potentials were recorded (Fig. 1B). The stimuli consisted of flashing spots and moving bars of various sizes. They were generated by a computer onto a monitor, which was imaged through an optical system and the condenser of the microscope onto the photoreceptor surface of the retina. The same stimuli were repeated on a slave monitor viewed during plotting of the receptive field.

We routinely recorded extracellular spikes larger (1 to 2 mV) than those usually encountered with metal electrodes, probably because we could optimally place the recording electrode near the cell. There was no sign of photodamage to the retina. The responses to light were brisk and stable for several hours. Even when we intentionally exposed the tissue to UV illumination for several minutes (a time period longer than we used for aiming the electrode), the ganglion cells were not irreversibly damaged. Because the electrode was placed visually, there was no doubt about which cell was recorded from, and DS cells later injected with Lucifer yellow all exhibited similar morphology (9).

Because of the stability offered by extracellular recording (the cells were usually studied for 1 to 2 hours), the receptive fields could be plotted in detail. Their directional preferences were independent of the contrast of the stimuli. When stimulated with a flashing spot, DS cells gave on-off transient responses. To plot the boundary of their receptive fields, we used both the traditional manual method and a computer-controlled automated method. For manual plotting, we used a computer mouse to move a flashing spot. We judged the boundary of the area within which a response could be evoked by listening to the response of the cell on an audiomonitor. For automated plotting, a flashing spot (usually 50 μm in diameter) was presented with 50-μm spacing across a large area covering the receptive field, and the number of spikes evoked at each location was averaged for five to ten trials. The border was drawn at the position where the response was 20% of the peak response evoked at the receptive field center (10). We found no significant difference in the receptive field boundaries obtained by these two methods.

After the receptive field had been plot-

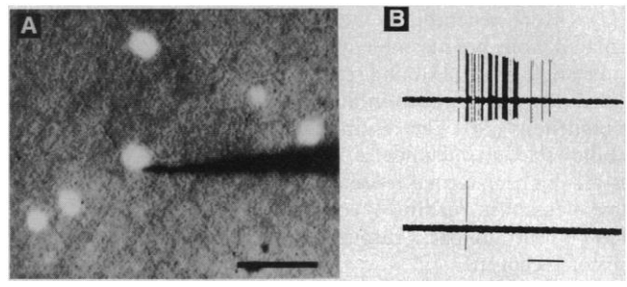

Fig. 1. (**A**) Video image of living retinal ganglion cells, retrogradely labeled after the injection of Fast blue into the optic nerve. The ganglion cell layer is facing upward. An intensified camera (Dage-MTI) with image processing (Image-1) was used to view the labeled cells, which fluoresce under blue-violet (355 to 425 μm) illumination. Under visual control, a tungsten-in-glass electrode was advanced toward a DS ganglion cell, tentatively identified by its medium-to-large cell body and smooth surface. The cell was confirmed as DS by subsequent physiological study. Scale bar, 50 μm. (**B**) Action potentials recorded from the DS cell. Only when the electrode was within about 10 μm of the cell body were large action potentials recorded. The cell shown in (A) was DS: it responded vigorously to a bar moving in the preferred direction (top trace) but gave weak responses to the bar moving in the opposite direction (lower trace). Scale bar, 100 ms.

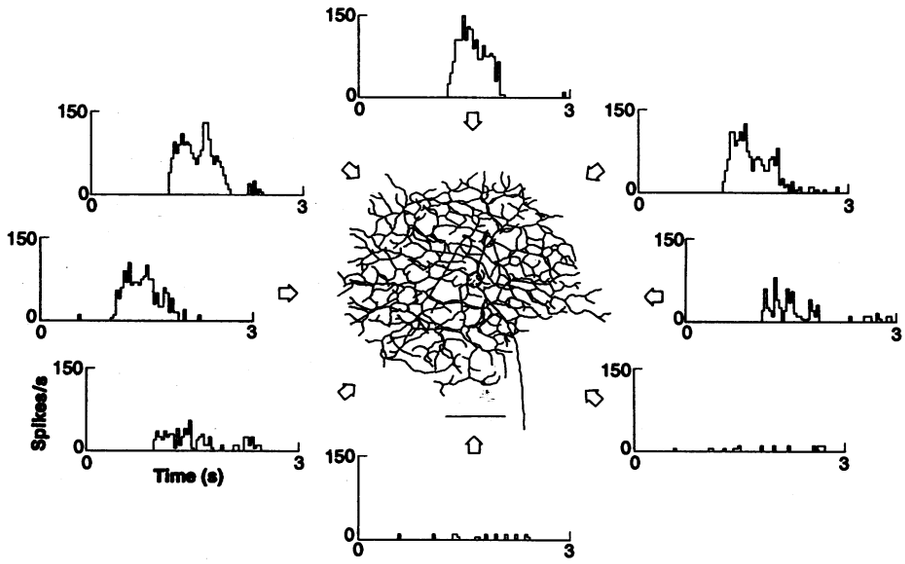

Fig. 2. Response histograms of an on-off DS cell to movements in different directions. Responses are expressed as spikes per second, averaged for five trials. Positioning of the electrode and subsequent intracellular injection of Lucifer yellow were performed under visual control. The arrows indicate the direction in which the test bar crossed the dendritic arbor of the cell shown. This cell has a bistratified dendritic tree (the two levels are collapsed onto a plane in the drawing). Its dendrites often curve backwards, forming a regular meshwork that covers the field uniformly. Scale bar, 100 μm.

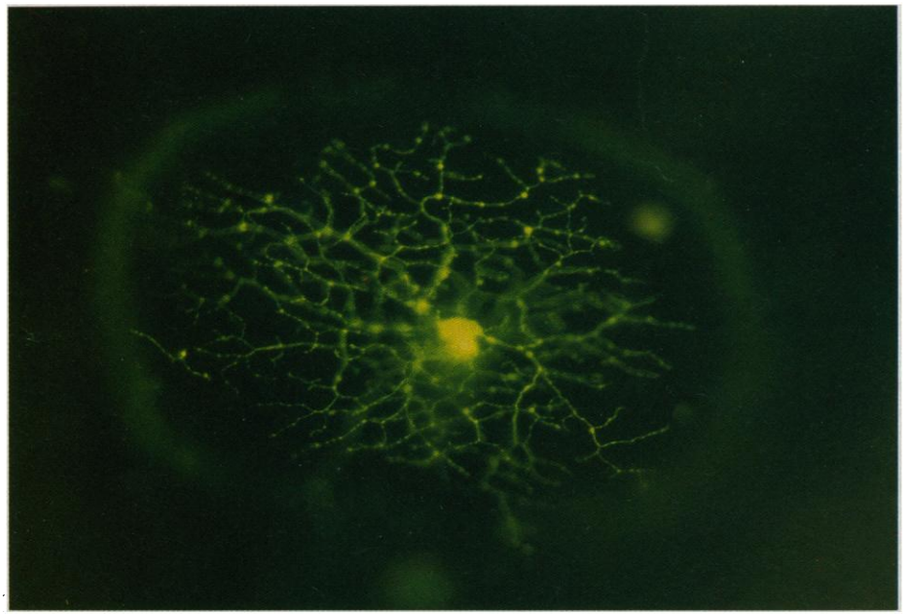

Fig. 3. Relation between the receptive and dendritic fields of a recorded DS cell. The micrograph was taken in the recording chamber immediately after the cell was injected. The faint ring surrounding the Lucifer yellow–filled cell is the boundary of the receptive field. It was drawn on a computer monitor used to plot the receptive field and projected through the same optical system onto the retina. The fuzziness of the receptive field boundary is due to scattering of light by the retina when the image is focused onto the photoreceptor side. The longest axis of the neuron's dendritic field covers 480 μm.

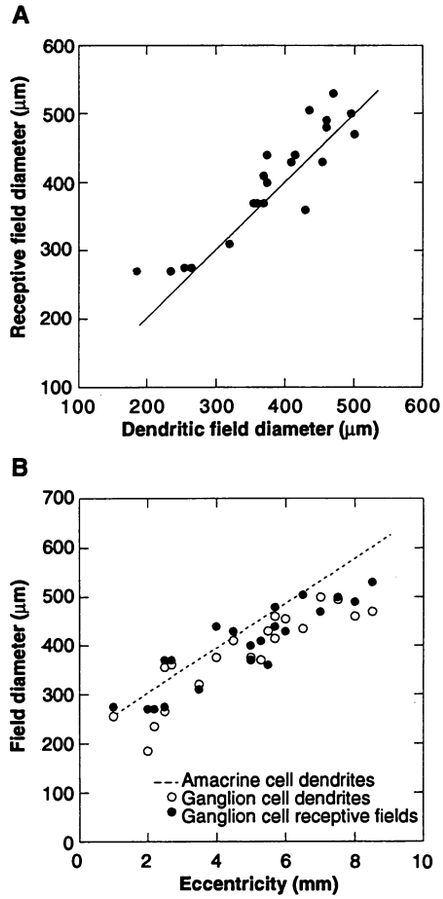

Fig. 4. (**A**) Scatter plot showing the correlation of receptive and dendritic field sizes of DS cells. The diameter expressed here is the average of the widest and narrowest diameters. The line shows the values expected if the receptive and dendritic fields were identical. (**B**) Relation of receptive and dendritic field sizes of DS cells and the dendritic fields of starburst amacrine cells at various retinal eccentricities. The data on the dendritic field size of the amacrine cells are from a previous study (*7*).

ted, the tungsten-in-glass electrode was withdrawn and replaced by a Lucifer yellow–filled micropipette, which was used to inject the cell under visual control. Because the ganglion cell bodies were labeled with Fast blue, the cell studied physiologically could be injected without ambiguity. We studied the physiology and morphology of 33 identified DS ganglion cells from both the central and peripheral retina. Figure 2 shows responses of an on-off DS cell to a bar moving at different directions in relation to its dendritic tree. The dendritic morphology confirms that reported by Amthor and colleagues in a smaller sample of cells from the central retina (*4*). We saw no obvious relation between the preferred directions of the DS cells and their dendritic morphology.

For a direct comparison of the receptive and dendritic fields, the boundary of the receptive field was drawn on the stimulus-generating monitor and projected onto the surface of the retina through the same optical system used for stimuli. This comparison was made for 21 cells. Figure 3 is a doubly exposed micrograph of a living retina, taken in the recording chamber, immediately after injection and without movement of the retina. The boundary of the receptive field is visible as a faint ring around the cell, just outside the tips of the Lucifer yellow–filled dendrites. In many instances the receptive field was almost perfectly concentric with the dendritic field (Fig. 3). In others it was shifted slightly to one side. It is not known whether the shifts have a consistent relation to the cell's physiology. In either case, however, the dendritic and receptive fields had nearly the same diameter.

The relation between the dendritic and receptive fields is shown in Fig. 4A. The receptive fields were similar to the dendritic fields at all retinal eccentricities. Figure 4B plots the diameters of the two fields as a function of retinal eccentricity. For comparison, the dendritic diameters of the starburst amacrine cells are also shown. The three diameters increase in parallel with the distance from the central retina.

These relations indicate that the overlapping starburst amacrine cells do not increase the size of the DS cell's receptive field. As mentioned previously, up to 70 overlapping starburst amacrine cells are present at any location on the retina (*7*). The overlapping starburst cells are believed to synapse on the DS cells at each location (*6*), and each starburst cell would be activated by light falling anywhere within its receptive field. Because the starburst cells' dendritic fields are roughly as wide as those of the DS cells, the region over which stimuli could affect the DS cell would be expected to have almost three times the diameter of the dendritic field of the DS cell. This is clearly not the case.

Five possibilities might be considered to explain why the overlapping starburst cells fail to increase the size of the DS ganglion cell's receptive field. (i) Segments of the dendrites of the starburst cells might be electrotonically isolated (*11*). However, Bloomfield (*12*) has shown that the starburst cells generate action potentials and these would conduct laterally. (ii) Dedicated starburst cells could be selectively connected to individual DS ganglion cells such that only the starburst cell directly superimposed on the dendritic field of the ganglion cell would synapse on it. This is unlikely because of the cofasiculation of the overlapping starburst dendrites (*13*). Moreover, such an arrangement would leave a "hole" in the middle of the ganglion cell's synaptic input because the starburst cells have outputs only in the distal third of their dendritic tree (*6*). (iii) The ganglion cell could perform a threshold operation, in which activity of the overlapping starburst

cells is summed. In this model, all of the overlapping starburst cells would excite the ganglion cells; for geometric reasons, the summed input to the DS cell would be greatest when the stimulus lies directly over the dendritic field of the DS ganglion cell. Such a mechanism seems implausible: a broad annulus presented around the DS cell's dendritic field would stimulate the ganglion cell because of the summed outputs of the neighboring starburst cells. (iv) Inhibitory inputs [from other retinal neurons or from the starburst cells' own release of γ-aminobutyric acid (GABA) (*14*)] could somehow negate the laterally conducted effects of the overlapping starburst cells. (v) The starburst cells could play a role other than the transmission of the information about moving stimuli. Whether one of these or some other possibility is correct, the discussion must clearly be reopened. Our results, together with those of Bloomfield (*12*), challenge the validity of all current models of retinal directional selectivity (*15*).

REFERENCES AND NOTES

1. H. B. Barlow and W. R. Levick, *J. Physiol.* **178**, 477 (1965).
2. C. W. Oyster, *J. Physiol. (London)* **199**, 613 (1968).
3. H. J. Wyatt and N. W. Daw, *J. Neurophysiol.* **38**, 613 (1975); V. Torre and T. Poggio, *Proc. R. Soc. London* **202**, 409 (1978); C. Koch, T. Poggio, V. Torre, *Philos. Trans. R. Soc. London* **298**, 227 (1982); L. Borg-Graham and N. M. Grzywacz, in *Single Neuron Computation*, T. McKenna, J. Davis, S. Zornetzer, Eds. (Academic Press, Boston, 1991).
4. F. R. Amthor, C. W. Oyster, E. H. Takahashi, *Brain Res.* **298**, 187 (1984); F. R. Amthor, E. H. Takahashi, C. W. Oyster, *J. Comp. Neurol.* **280**, 97 (1989).
5. R. H. Masland and J. W. Mills, *J. Cell Biol.* **81**, 159 (1979); R. H. Masland and A. Ames III, *J. Neurophysiol.* **39**, 1220 (1976).
6. E. V. Famiglietti, *J. Neurosci.* **309**, 40 (1991).
7. M. Tauchi and R. H. Masland, *Proc. R. Soc. London Ser. B* **223**, 101 (1984); D. I. Vaney, *ibid.* **220**, 501 (1984).
8. The methods used were those developed by Ames and colleagues [A. Ames and F. B. Nesbett, *J. Neurochem.* **37**, 867 (1980); (*5*)]. For injection of Fast blue, the rabbit was anesthetized with a combination of Nembutal and ether, the eye was protopsed, and 10 μl of 1% Fast blue was injected into the nerve through a slit in the conjunctiva. For isolation of the retina, the animal was again anesthetized, the eye removed, and the animal killed by an overdose of Nembutal without waking from anesthesia. The eye was everted under Ames medium, and the retina gently teased away from the pigment epithelium. Subsequent incubation and maintenance in vitro were as described (*5*).
9. This method combines the advantages of extracellular recording (intracellular recordings in rabbit retina are difficult and brief) with identification of the recorded cell, which usually requires intracellular recordings. It can also be used for the study of infrequently occurring types of cells in retina or in other neural tissues because it solves the problem of sampling bias that may occur with metal electrodes [W. R. Levick and L. N. Thibos, *Prog. Retinal Res.* **2**, 267 (1983)].
10. The boundaries estimated by flashing spots were nearly the same as those established with moving spots (in the preferred direction). The roll-off at the edges of a DS cell's receptive field is apparently sharper than that of the α and β cells [L. Peichl and H. Wassle, *J. Physiol.* **291**, 117 (1979)], making it relatively easy to determine the receptive field boundaries in DS cells. The boundary described here is for small spots flashed within the receptive field or moved across its edges. Under special conditions, an inhibitory region extending beyond the on-off zone of these cells has been demonstrated (*1*, *2*).
11. R. H. Masland, J. W. Mills, C. Cassidy, *Proc. R. Soc. London Ser. B* **223**, 121 (1984); R. H. Miller and S. A. Bloomfield, *Proc. Natl. Acad. Sci. U.S.A.* **80**, 3069 (1983).
12. S. A. Bloomfield, *Nature* **350**, 347 (1991); *J. Neurophysiol.* **68**, 711 (1992); *Invest. Ophthalmol. Visual Sci.* **33**, 1173 (1992).
13. E. V. Famiglietti, *Brain Res.* **261**, 138 (1983); M. Tauchi and R. H. Masland, *J. Neurosci.* **5**, 2494 (1985); C. Brandon, *Brain Res.* **401**, 385 (1987); D. I. Vaney, S. P. Collin, H. M. Young, in *The Neurobiology of the Inner Retina*, R. Weiler and N. Osborne, Eds. (Springer-Verlag, Berlin, 1989), p. 154.
14. M. Ariel and N. W. Daw, *J. Physiol. (London)* **324**, 161 (1982); N. Brecha *et al.*, *Proc. Natl. Acad. Sci. U.S.A.* **85**, 6187 (1988); T. Kosaka *et al.*, *Exp. Brain Res.* **70**, 605 (1988); D. I. Vaney and H. M. Young, *Brain Res.* **438**, 369 (1988); D. M. O'Malley and R. H. Masland, *Proc. Natl. Acad. Sci. U.S.A.* **86**, 3414 (1989); D. I. Vaney, *Prog. Retinal Res.* **9**, 1 (1990).
15. A model by Borg-Graham [thesis, Massachusetts Institute of Technology (1991)] points out that many amacrine cells can have the asymmetry necessary for a DS input to the ganglion cells. To carry out this function, however, the postulated non-starburst amacrine must (i) have a density and dendritic spread similar to that of the starburst cell; (ii) lie on a direct excitatory pathway to the DS cell; (iii) generate no action potentials; and (iv) have a suitably short electrotonic length constant. No other known amacrine cell meets even the first two of these requirements.

16. Supported by NIH grant R37-EY01075. We thank M. Beauchamp for assistance with the stimulus-generating program.

23 June 1992; accepted 25 September 1992

Cloning of a Delta Opioid Receptor by Functional Expression

Christopher J. Evans,* Duane E. Keith Jr., Heather Morrison, Karin Magendzo, Robert H. Edwards

Opiate drugs have potent analgesic and addictive properties. These drugs interact with receptors that also mediate the response to endogenous opioid peptide ligands. However, the receptors for opioids have eluded definitive molecular characterization. By transient expression in COS cells and screening with an iodinated analog of the opioid peptide enkephalin, a complementary DNA clone encoding a functional δ opioid receptor has been identified. The sequence shows homology to G protein–coupled receptors, in particular the receptors for somatostatin, angiotensin, and interleukin-8.

Opiate drugs such as morphine affect the perception of pain, consciousness, motor control, and autonomic function by interacting with specific receptors expressed throughout the central and peripheral nervous systems (*1*). The endogenous ligands of these opiate receptors have been identified as a family of more than 20 opioid peptides that derive from the three precursor proteins proopiomelanocortin, proenkephalin, and prodynorphin (*2*). Although the opioid peptides belong to a class of molecules distinct from the opiate alkaloids, they share common structural features including a positive charge juxtaposed with an aromatic ring that is required for interaction with the receptor (*3*).

C. J. Evans, D. E. Keith, Jr., K. Magendzo, Department of Psychiatry, University of California at Los Angeles School of Medicine, Los Angeles, CA 90024–1759.
H. Morrison, Departments of Neurology and Microbiology and Immunology, University of California at Los Angeles School of Medicine, Los Angeles, CA 90024–1769.
R. H. Edwards, Department of Neurology and the Molecular Biology Institute, University of California at Los Angeles School of Medicine, Los Angeles, CA 90024–1769.

*To whom correspondence should be addressed.

Classical pharmacological studies have defined three classes of opioid receptors—δ, μ, and κ that differ in their affinity for various opioid ligands and in their distribution (*4*). The δ receptors bind with the greatest affinity to enkephalins and have a more discrete distribution in the brain than either μ or κ receptors, with high concentrations in the basal ganglia and limbic regions. Although morphine interacts principally with μ receptors, peripheral administration of this opiate induces release of enkephalins (*5*). Thus, enkephalins may mediate part of the physiological response to morphine, presumably by interacting with δ receptors. Despite pharmacological and physiological heterogeneity, the three types of opioid receptors inhibit adenylyl cyclase, increase K^+ conductance, and inactivate Ca^{2+} channels through a pertussis toxin–sensitive mechanism. These results and others suggest that opioid receptors belong to the large family of cell surface receptors that signal through G proteins (*6*).

Previous reports have described the isolation of two cDNAs that may function as opiate receptors. The sequence of a cDNA